Biomedical Materials

PAPER

A three-layered hollow tubular scaffold as an enhancement of nerve regeneration potential

Biomedical Materials

PAPER

A three-layered hollow tubular scaffold as an enhancement of nerve regeneration potential

Nasim Golafshan, Mahshid Kharaziha and Morteza Alehosseini

Department of Materials Engineering, Isfahan University of Technology, Isfahan 84156-83111, Iran

E-mail: kharaziha@cc.iut.ac.ir

RECEIVED
11 April 2018

REVISED
27 July 2018

ACCEPTED FOR PUBLICATION
8 August 2018

PUBLISHED
24 August 2018

Keywords: Three-layered scaffolds, nerve guidance conduit, electrical stimulation, graphene

Supplementary material for this article is available online

Abstract

A significant clinical challenge in the surgery of peripheral nervous system injured via accidents and natural disease is development of biomimetic grafts which could potentially promote nerve repair and regeneration. Although various engineered neural tissue scaffolds have been proposed to support the neural cell functions, they have not been able to instantaneously mimic the whole characteristics of endogenous microenvironment. In this study, we proposed a three-layered tubular scaffold which could provide appropriate electrical, mechanical and biological properties for peripheral nerve engineering. While the inter layer was graphene (Gr) embedded alginate-polyvinyl alcohol (AP-Gr) fibrous scaffold with well-defined anisotropy, the outer layer was double network scaffold of polycaprolactone fumarate (PCLF) and eggshell membrane (ESM). These two layers were attached together using a polycaprolactone (PCL) fibrous membrane, a middle layer, via a simple melting process. Results showed that while the electrical conductivity of the three-layered scaffold was similar to that of AP-Gr fibrous layer, the strength of the three-layered scaffold was significantly improved compared to AP-Gr and ESM-PCLF (1.5 and 1.1 times, respectively) attributed to well attachment of the two layers. As a proof-of-concept, PC12 cell attachment, proliferation, and alignment were studied on the developed three-layered scaffold. The majority of the cells (55%) aligned ($<20^{\circ}$) along the major axis of fibers features. Furthermore, electrical stimulation revealed positive effect on the alignment of PC12 cells and change in the cell morphology. With the ease of fabrication and mechanical robustness, the three-layered scaffold of AP-Gr and ESM-PCLF might be utilized as a versatile system for the engineering of peripheral nerve tissue.

1. Introduction

For a long period of time, peripheral nerve injuries experienced in transportation accidents and natural disasters have been a meaningful worry to human life all over the world owning to the inadequate capacity of nerves to repair after damage. Peripheral nerve trauma which is larger than 5 mm is no longer an option to cure by intestinal anastomosis as it creates detrimental tension along the nerve and postpones healings. In such situations, to afford better regenerative results, interfering a graft between the distal and proximal of the nerve cable could be a promising curing method (Xie *et al* 2014). Presently, few successful approaches are available to endorse peripheral nerve regeneration and functional rescue (Isaacs and Browne 2014). Although autologous nerve grafting is a gold standard, donor site morbidity, additional surgeries, scar tissue formation, and neuroma formation result in the development of tissue engineering. Tissue engineered nerve scaffolds based on various types of polymers have been developed to repair and regenerate peripheral nerve damages (Nectow *et al* 2012).

In order to provide effective nerve regeneration, scaffolds need to provide appropriate physical and chemical characterizations consisting of biocompatibility, biodegradability, physiologically appropriate flexibility and mechanical properties, anisotropic structure, hydrophilicity to encourage cell interaction and be semi-permeable (Xie *et al* 2014, Zou *et al* 2016, Ryan *et al* 2017). Moreover, the scaffolds need to be porous. Macropores with several hundreds of

micrometers were suitable for cell migration and neovascularization of a scaffold *in vivo* (Li *et al* 2013), while micropores were highly effective on delivery of nutrients, oxygen, and chemical cues that promoted cell function and fast healing (Jiang *et al* 2014). Moreover, the scaffolds should be electrical conductance, and provide contact guidance via tubular three-dimensional (3D) structure (O'Brien 2011). To provide these properties, nerve guidance conduits made of natural polymers such as collagen (Sulong *et al* 2014), eggshell membrane (ESM) (Golafshan *et al* 2017a), sodium alginate (Golafshan *et al* 2017b), hyalouronic acid (Mekaj *et al* 2015) as well as biodegradable synthetic polymers such as polycaprolactone fumarate (PCLF) (Wang *et al* 2009), polyvinyl alcohol (PVA) (Naghavi Alhosseini *et al* 2015, Golafshan *et al* 2017c) and polycaprolactone (PCL) (Lee *et al* 2012) have been developed. In this way, in order to induce electrical conductance to promote neural and axonal regeneration, conductive nanoparticles such as carbon nanotubes (Amini *et al* 2013), gold nanoparticle (Lin *et al* 2008), graphene oxide (Liu *et al* 2017) and electrically conductive polymers such as polypyrrole (PPy) (Zou *et al* 2016) were applied. Results revealed that these conductive constructs could improve neuron interaction via supporting and encouraging the neural regeneration following the damage (Zhang *et al* 2016, Zou *et al* 2016, Liu *et al* 2017). One of the most interesting substrates which mimics the hierarchical structure of the extracellular matrix (ECM) is a fibrous substrate (Alehosseini *et al* 2018). Recently, we developed alginate-PVA:Gr (AP-Gr) scaffolds and revealed that AP-Gr scaffolds presented excellent electrical and mechanical characteristics with superior PC12 cell interaction (Golafshan *et al* 2017b). Although this class of constructs are high compatible for peripheral nerve tissue engineering, they interface with some issues consisting of surgical handling, scarce cell infiltration and nutrient, inability to provide 3D structures, and inadequate mechanical properties (Khorshidi *et al* 2016).

To overcome these issues, three-layered constructs consisting of fibrous structures as inter layers have been proposed (Zhu *et al* 2011, Mottaghitalab *et al* 2013, Xie *et al* 2014). In these structures, outer layers not only should be mechanical robust but also must provide porous structure with enough tissue adhesion to help neural tissue regeneration (Kakinoki *et al* 2014, Xie *et al* 2014). To provide these properties, ESM as a super hydrophilic, biocompatible and porous material could be a promising candidate. Thanks to the suitable chemical and structural properties of ESM, it could be a favorable for nerve tissue engineering. However, the application of ESM has been restricted due to its weak mechanical behavior. Recently, we developed double network system of PCLF and ESM by using the vacuum infiltration method. Compared to ESM, the toughness and strength of the double-network scaffold were meaningfully enhanced (26 and 13 times, respectively) making it suitable for nerve tissue engineering applications (Balaz 2014, Golafshan *et al* 2017a).

In the present work, we developed three-layered tubular structure based of aligned fibrous AP-Gr scaffold as the inter layer and a double-network membrane of ESM-PCLF as the outer layer. While aligned fibrous AP-Gr scaffold acted as the guidance for cells and provide electrical conductivity, the double-network system was served as a tear-resistant and mechanically robust construct. This new type of nerve guidance conduit was fabricated by adhesion and rolling these layers into a tube with a facile and unprecedented method.

2. Experimental section

2.1. Materials

Sodium alginate (SA) from brown algae with medium viscosity, polyvinyl alcohol (PVA, Mw = 72 000), poly(caprolactone-diol) (PCL-diol, Mn = 2000), polycaprolactone (PCL), glutardehyde 25% (GA), bisacylphosphinoxide (BAPO), Triton X-100™, dimethyl sulfoxide (DMSO) and tetrahydrofuran (THF) were provided from Sigma-Aldrich Co. Chloride calcium ($CaCl_2$), glycerol ($C_3H_8O_3$), and acetic acid were provided from Merck Co. Pristine graphene (less than 32 Layers, purity >99.5%) purchased from Nanosany Co. PC12 cells were obtained from the Pasteur Institute, Iran (NCBI code: C153) for cell culture studies. Dulbecco's Modified Eagle's Medium Hi-glutamine (DMEM-HI), trypsin-EDTA, antibiotics and phosphate buffered saline (PBS) were taken from Bioidea, Iran. Fetal bovine serum (FBS) was purchased from GIBCO, and horse serum (HS) was obtained from Bahar Afshan, Iran. Resazurin, MTT (3-(4,5-Dimethylthiazol-2-yl)-2,5-diphenyltetrazolium bromide), paraformaldehyde (PF) and DAPI (40,6-diamidino-2-phenylindole) were gotten from Sigma Aldrich Co. Rhodamine phalloidin was provided from cytoskeleton, USA. In all the experimental sections, double distilled water was used.

2.2. Fabrication of three-layered tubular scaffolds

The methodology to fabricate the three-layered scaffold was divided into two distinct stages. The first stage was the fabrication of the nerve conduit's components, including aligned fibrous alginate-PVA:Gr (AP-Gr) scaffold as the internal layer, the double network system of ESM-PCLF membrane as outer layer, and random fibrous PCL membrane as the adhesive layer. The second stage was the assembly of these layers and rolling the three-layered scaffold to fabricate tubular three-layered structure.

Aligned fibrous AP-Gr scaffold consisting of 1 wt% Gr was developed using electrospinning technique, according to our previous research (Golafshan *et al* 2018). Briefly, alginate:PVA solution with volume ratio of 80:20 was prepared in distilled water consisting of glycerol (0.75%(v/v)) and Triton X-100

(0.5 wt%). After addition of 1 wt% Gr to the polymeric solution, the polymer suspension was sonicated for 30 min (WUDD10H, Power 770 W) at room temperature and subsequently fed into a 1 ml syringe having a 23 G blunted stainless steel needle. Electrospinning process was performed at constant voltage of 18 kV, flow rate of 0.12 ml h^{-1}, and the tip to the collector distance of 10 cm. In order to fabricate aligned fibrous scaffold, a wire drum collector with the speed of 800 rpm was established to organize fibers. The crosslinking process was performed in two steps; crosslinking of PVA using glutaraldehyde (GA) solution in methanol and acetone with volume ratio of 10:4, and crosslinking of alginate via soaking in 2 wt% $CaCl_2$ solution in ethanol for 1 h. Finally, the scaffolds were immersed in PBS to remove non-crosslinked chains. Afterward, the scaffolds were immersed in water for 2 d to wash GA.

ESM-PCLF membrane was fabricated according to our previous research (Golafshan *et al* 2017a, Golafshan *et al* 2018). Briefly, ESM from hens' egg was washed with double distilled water to remove albumen and consequently soaked in 10 wt% PCLF solution in acetic acid containing 5 wt% bisacylphosphinoxide (BAPO) as the photo-initiator. Finally, vacuum infiltration was performed to remove air from the ESM pores and facilitate penetration of PCLF solution into those pores.

To adhere two layers including aligned AP-Gr scaffold and ESM-PCLF membrane, a thin layer of fibrous PCL membrane fabricated using electrospinning process (working distance of 15 cm, flow rate of 0.12 ml h^{-1} working, voltage of 15 kV), was used as a binder. PCL fibrous membrane was placed on the top of aligned fibrous AP-Gr scaffold which primarily was brushed with THF in a petridish. Consequently, the ESM-PCLF layer was layered above and the two-layered membrane. Three layers of AP-Gr scaffold: PCL:ESM-PCLF were maintained together and pushed under a pressure about 0.1 MPa using a weight on the top of three layers at 80 °C for 30 min to melt PCL membrane, while AP-Gr scaffold and ESM-PCLF membrane remained stable. Finally, the scaffold was cooled at room temperature. During solidification, the PCL layer acted as a binder by entrapping the fibers of AP-Gr and ESM-PCL membranes.

2.3. Characterizations of three-layered scaffolds

To evaluate detailed fiber and tubular morphologies, a scanning electron microscope (SEM) (Philips, XL30) was used at an accelerating voltage of 10 kV. The samples were coated with a gold sputtering for 400 s. The diameter of 30 fibers for AP-Gr scaffold, ESM-PCLF, and PCL membrane were measured manually using ImageJ software (NIH, USA). Additionally, 30 pores per sample type were measured ($n = 3$) to calculate the average pore size. Besides, the distribution of Gr nanosheets in the AP-Gr fibers was assessed by transmission electron microscopy (Philips EM208S 100 kV). The chemical composition and functional group of prepared three-layered scaffold was studied by means of a Jasco-680 Fourier transform infrared (FTIR) spectrophotometer (Japan) using 8 mm s^{-1} scan rate as well as x-ray diffraction (XRD, X0 Pert Pro x-ray diffractometer, Phillips, Netherlands) technique carried out with CuKa radiation ($\lambda = 0.154$ nm) at a generator voltage of 40 kV and a current of 40 mA.

The uniaxial tensile properties of the three-layered scaffold were estimated using uniaxial tensile tester machine (Hounsfield H25KS) with cell load capacity of 10 N at the rate of 3 mm min^{-1} at wet condition. Five specimens, with 40 mm in length and 10 mm in width, were used for each scaffold and immersed in PBS for 2 h at room temperature, before mechanical testing. The stress–strain curves were plotted and energy per volume (toughness), strength, and elastic modulus were obtained. To evaluate the electrical conductance of three-layered scaffolds, electrical impedance was applied for sample with the dimension of 20 mm × 20 mm ($n = 3$) using PARSTAT 2273, USA electrochemical workstation. 2 M H_2SO_4 solution used for this assay which three-electrode system consisting of an Ag/AgCl, a platinum electrode as the reference electrode, counter electrode respectively, and sample as reference electrode over 1.0 MHz–10 Hz at room temprature.

2.4. Cell culture

The biological properties of the three-layered scaffold were investigated using PC-12 cells (institute Pasteur, Iran) expanded in growth media (DMEM-Hi supplemented with 10% FBS, 5% HS, and 0.1% penicillin/streptomycin). After sterilization of the samples via 30 min soaking in 70% (v/v) ethanol and exposure to ultraviolent (UV) light for 2 h, they were subsequently immersed in complete culture medium overnight, prior to cell seeding in 24-well plates. Consequently, PC12 cells were seeded on them ($n = 3$) with a density of 2×10^4 cells/well and incubated for 14 d at 37 °C in 5% CO_2 condition. During cell culture, the media was changed every two days.

2.4.1. Electrical stimulation of cultured PC12 cells

Electrical stimulation was applied to the cell-seeded scaffolds every 2-day period using an electrical stimulation setup consisting of two carbon rod electrodes which the copper wire was rolled at the opposite end of the electrodes and were fixed by silicon adhesive. Prior to electrical stimulation, the chamber was washed with 70% ethanol for 1 h and exposed to UV radiation. 24 h after cell seeding, the cell-seeded scaffolds were placed

between two parallel carbon rod electrodes and the petri-dish was filled with 25 ml growth media to cover the constructs and both electrodes. Consequently, electrical stimulation was performed at a steady potential of 0.5 V and 0.03 mA for a period of 60 min.

2.4.2. The viability, attachment, metabolic activity and morphology of cultured PC12 cells

The viability of PC12 cells seeded on the three-layered scaffolds compared to that of on the AP-Gr scaffold and tissue culture plate (TCP) was assessed using MTT assay. After specific time point, the cell-seeded samples were incubated in 0.5 mg ml^{-1} MTT solution in PBS for 4 h. Consequently, in order to dissolve the violet formazan crystals, 500 μl DMSO was added to each sample and kept for 25 min on shaker. Finally, the optical density was determined at 490 nm in a microplate reader (BioTek, Model ELX800 Instruments). All experiments were performed in triplicate and the relative cell viability (%) was reported as a percentage relative to the control sample.

The proliferation of cells seeded on the three-layered and AP-Gr scaffolds as well as TCP was studied using Resazurin assay ($n = 3$) at the specific time points. After discarding the complete media from scaffolds, Resazurin solution with the concentration of 10 $\mu g\,ml^{-1}$ in complete medium was added to each sample and kept in incubator for 4 h, until the color of the resazurin solution was changed. Subsequently, after transforming to the 96-well plate, the absorbance of solutions and complete media (control) were recorded in 630 nm using microplate reader.

The morphology of PC12 cells cultured on the scaffolds after 7 d of culture was evaluated by SEM images. After 3 h fixation with 2.5 (v/v)% glutaraldehyde in 4 °C, the samples were rinsed with PBS, and dehydrated in the gradient concentrations of ethanol (30, 70, 90, 96 and 100 (v/v)%) for 10 min, respectively. Finally, they were placed in a desiccator, gold-coated and evaluated using SEM imaging. Moreover, to evaluate the surface of the samples covered with PC12 cells, the samples were analyzed by ImageJ software. For this purpose, three images were chosen and the total areas covered with PC12 cells was determined.

2.4.3. Immunostaining for cell cytoskeletal organization

Immunostaining was performed to assess the role of electrical stimulation on the cytoskeletal organization (F-actin) of PC12 seeded on the samples. The cell-seeded samples were fixed using 4% (v/v) PF for 2 h, permeabilized in 0.1% Triton X-100 for 5 min, and, finally, incubated with 2% (v/v) bovine serum albumin in PBS for 1 h to reduce nonspecific background staining. Consequently, after twice rinsing with warm PBS, PC12 cells were incubated with 1:40 dilution of rhodamine phalloidin (cytoskeleton, USA) solution for 30 min to stain actin filaments. Consequently, the cells' nuclei were stained with 1:1000 dilution of 40, 6-diamidino-2-phenyl indole dihydrochloride (DAPI, sigma-Aldrich, Germany) in PBS for 5 min. Finally, the stained samples were imagined using a fluorescence microscope (Nikon TE 2000-U, Nikon instruments Inc., USA). Moreover, to quantify cellular alignment on the three-layered scaffolds and TCP (control), florescence images were obtained at two to three different locations of each sample. The normalized cellular alignment angles were finally grouped in 0°–20° increments to compare the alignment of PC12 cells on the three-layered scaffolds and TCP.

2.4.4. Mechanical evaluation of PC12 cell-seeded scaffolds

The mechanical properties of the cell-seeded scaffolds were also evaluated using tensile test. In this way, three-layered scaffolds with the size of 40 mm × 10 mm were seeded using 3×10^5 PC12 cells and incubated in six-well plate for 2 weeks. Consequently, unseeded and PC12-seeded scaffolds were tensile tested as described previously, using uniaxial tensile tester machine (Hounsfield H25KS) with load of 10 N at the rate of 3 mm min^{-1}. Finally, elastic modulus (E), tensile strength, and toughness were measured.

2.5. Statistical analysis

Statistics analysis was achieved by Graphpad PRISM 7 and all the values were averaged in triplicate specimens and presented as means ± standard deviation. Significant differences were determined by One-Way ANOVA analysis and it was considered as statistically significance at $p < 0.05$.

3. Results and discussion

3.1. Characterization of three-layered scaffolds

According to figure 1(A), to regenerate injured peripheral nervous system, guidance conduits are designed to bridge injured sites and provide a physical template for the regeneration of peripheral nerves (Lackington *et al* 2017). In order to stimulate the regeneration of damaged peripheral nerve tissue, in this study, three-layered tubular construct was developed using aligned fibrous AP-Gr scaffold (inner layer) and ESM-PCLF scaffold (outer layer) attached via PCL fibrous intermediate layer (figure 1(B)). This three-layered construct was finally rolled to form tubular structure.

According to figure 2(A) the three-layered structure with the tubular morphology and the outer diameter of 1.6 mm was successfully achieved by rolling the membrane. Cross-section of tubular structure (figure 2(B)) clearly showed that the three-layered

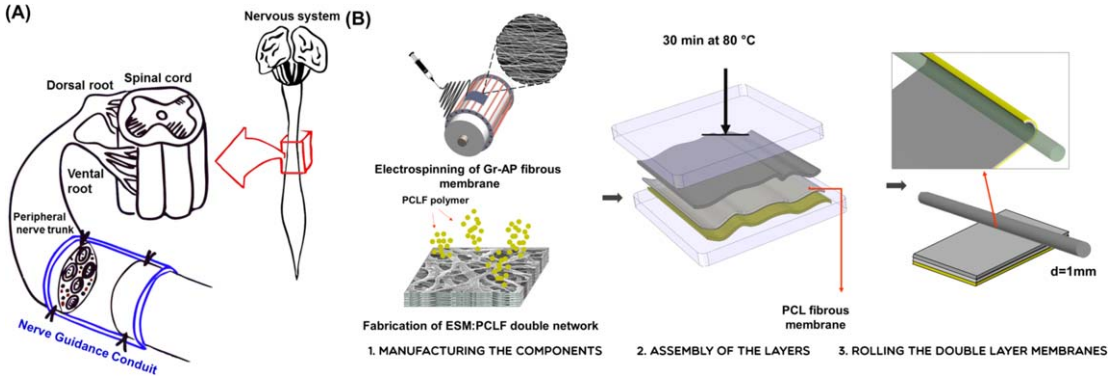

Figure 1. (A) Schematic representation of peripheral nerve systems and surgical implantation of nerve guidance conduit for broken nerve trunk. (B) The schematic of the three-layered scaffold fabrication process consisting of three steps: (1) preparation of components including AP-Gr, ESM-PCLF and PCL layers, (2) attaching two layers by a simple melting process using the PCL fibrous membrane (thermoplastic mat) under pressure and temperature and (3) rolling the three-layered scaffold using a copper wire ($d = 1$ mm).

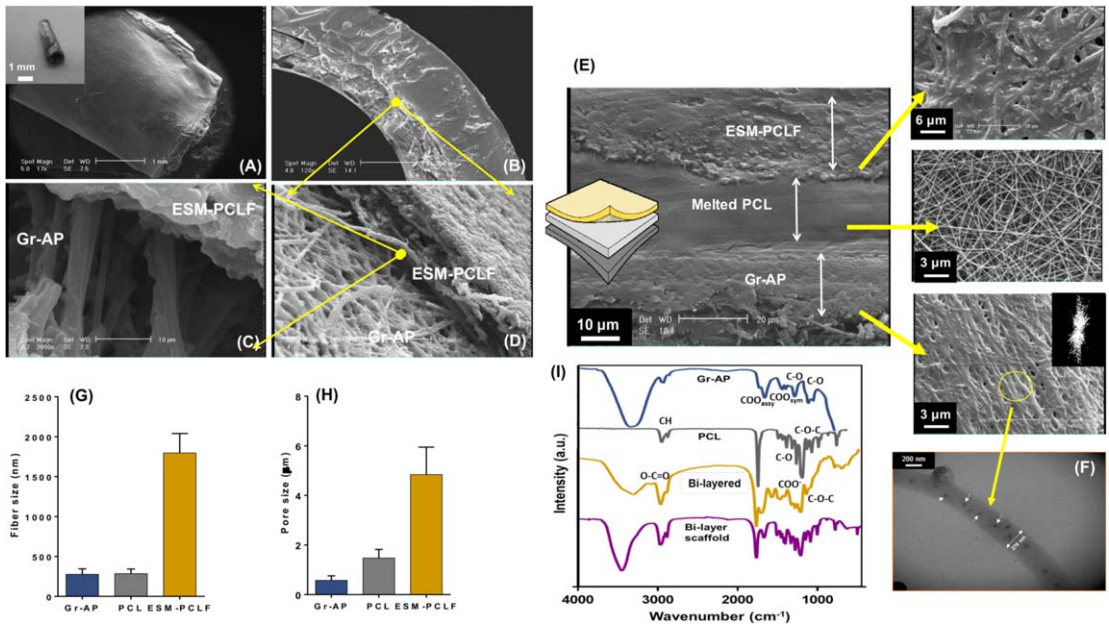

Figure 2. Structural properties of the three-layered scaffold: (A) SEM images of nerve guidance conduit consisting of AP-Gr as the inner layer and ESM-PCLF as the outer layer. (B) The cross-section of nerve guidance conduit represented two distinct layers of the scaffold: (C) AP-Gr (inner layer) and (D) ESM-PCLF (outer layer) of nerve guidance conduit. (E) A magnified cross-sectional view of the three-layered scaffold and the morphology of each layer (scale bar $= 3$ μm). (F) TEM image of AP-Gr scaffold showing the well distribution of Gr within the fibrous structure. (G) Fiber and (H) pore size of each layer of the scaffold. (I) FTIR spectra of AP-Gr, PCL, ESM-PCLF, and three-layered scaffolds.

construct with thickness of 285.1 $\pm$ 20 μm consisted of three distinguished layers. Moreover, between various layers, the outer layer (ESM-PCLF membrane) revealed the greatest thickness (176.6 $\pm$ 11 μm), while the porosity of the inner layer (AP-Gr scaffold with thickness of about 100.1 $\pm$ 6 μm) was the highest. This structure could be helpful in the nerve conduit to maximizing nutrient diffusion and also serves to facilitate mechanical interlocking between the conduit and surrounding tissue to improve the mechanical stability of the conduit and regenerating nerve tissue effectively (Loh and Choong 2013). Moreover, higher magnification images (figures 2(C) and (D)) showed that the scaffold consisted of two distinct layers: aligned fibrous scaffold as an internal layer (AP-Gr) and a double network scaffold as an external layer (ESM-PCLF). Figure 2(E) also exhibited that the melted fibrous PCL with thickness of 19.1 $\pm$ 1 μm penetrated to the pores of two layers. It is clear that AP-Gr and ESM-PCLF integrated truly and firmly adhered to each other by melted PCL electrospun fibers. The surface morphology of each layer is presented in figure 2(E). AP-Gr layer consisted of aligned fibers with the orientation index of OI $= 28.7^{\circ}$ which was

closely mimic that of native nerve fiber with OI = 26.8°. This morphology could be helpful for proliferation of neural cells and axon regrowth. TEM image of aligned fibrous AP-Gr layer (figure 2(F)) showed the presence of graphene nanoparticles with size of 88 ± 13 nm which uniformly dispersed into the polymeric matrix to provide hybrid material with high performance and certain functionalities. Furthermore, PCL layer which acted as binder revealed the smooth fibers with the average fiber and pore size of 284 ± 58 μm and 1.5 ± 0.3 μm, respectively. Moreover, ESM-PCLF membrane consisted of inner ESM as a platform which incorporated by PCLF polymer solution. After incorporation PCLF, the pore size decreased to 4.8 ± 1.1 μm leading to promoted mechanical properties of ESM. According to SEM images, the fiber and pore sizes of each layers were estimated (figures 2(G) and (H)). Between various layers, ESM-PCLF membrane revealed the noticeably greatest fiber size (1796.2 ± 244 nm) and pore size (4.8 ± 1.1 μm).

To confirm the formation of three-layered construct, FTIR spectroscopy was performed (figure 2(I)). FTIR spectrum of AP-Gr scaffold consisted of the characteristic absorption bands of PVA at 849, 1096, 1336, 1440, and 2944 cm^{-1} and sodium alginate appeared at 1615, 1417, and 3430 cm^{-1}. Furthermore, PCL fibrous membrane consisted of carbonyl stretching (C=O) (at 1727 cm^{-1}), symmetric C–H stretching (at 2863 cm^{-1}), asymmetric C–H stretching (at 2950 cm^{-1}), asymmetric C–O–C stretching (at 1240 cm^{-1}) and C–O and C–C stretching (at 1293 cm^{-1}) related to the main characteristic peaks of PCL. Moreover, FTIR spectrum of ESM-PCLF consisted of the strong bands at 1726 cm^{-1} (skeletal ester), 1170 cm^{-1} (ether stretches) and 1105 cm^{-1} (vibration of COO^- and C–O–C groups) related to PCLF component. Moreover, the characteristic bands of ESM could be detected at 3310 cm^{-1} (attributed to the O–H and N–H stretching mode), 3064 cm^{-1}, 2935 cm^{-1}, and 2870 cm^{-1} (corresponded to the asymmetric stretching vibrations of the C–H bonds presented in =C–H and $=CH_2$ groups), 1648 cm^{-1} (due to the C=O stretch of amides), 1525 cm^{-1} (attributed to the CN stretching NH bending modes), and 1234 cm^{-1} (corresponded to the CN stretching/NH bending modes). The last three peaks can be assigned to the amide I (1648 cm^{-1}), amide II (1525 cm^{-1}), and amide III (1234 cm^{-1}) vibrations of the glycoprotein mantle of ESM, respectively. FTIR spectrum of three-layered scaffold consisted of the characteristic peaks related to the component of construct. Results confirmed that heat-treatment process did not have noticeable effect on the chemical structure of each component. Moreover, it could be concluded that the bonding between the layers did not result in the formation of new compounds. XRD patterns of the scaffolds were also studied to investigate their chemical composition. According to the figure S1 (available online at stacks.iop.org/BMM/13/065005/mmedia), AP-Gr scaffold consisted of a sharp peak around 27° owing to the interaction of Gr nanoparticles with PVA and alginate blend. XRD pattern of ESM-PCLF membrane revealed a broad diffraction peak at $2\theta = 21.1°$ confirming its amorphous characteristic. However, the XRD pattern of PCLF revealed some crystalline characteristic peaks related to PCLF polymer. According to previous research (Wang *et al* 2008), PCLF showed the diffraction peaks at $2\theta = 20.2°$ and 23.7° as its precursor PCL diols. Such these peaks at XRD pattern of three-layered scaffold overlapped each other on and revealed like a broad diffraction peak.

To evaluate the effect of multi-layering and the interaction between these layers on the mechanical properties of the construct, uniaxial tensile test was carried out compared with each single layer of AP-Gr and ESM-PCLF, after submerged in PBS for 2 h. All stress–strain curves of the scaffolds (figure 3(A)) showed that, as strain gradually increased, the curves deviated from the linear region proportionality and exhibited significant changes on the mechanical properties. According to figure 3(A), binding of two layers using PCL fibrous membrane resulted in development of the three-layered scaffold with significant improvement of mechanical properties such as elastic modulus, strength, and elongation. According to the stress–strain curves, elastic modulus, toughness, and tensile strength of the single layers and three-layered scaffolds were calculated and presented in figures 3(B)–(D). Between them, the three-layered scaffolds composed of AP-Gr scaffold and ESM-PCLF membrane exhibited the strongest construct (1.5 and 1.1 times greater in strength compared AP-Gr and ESM-PCLF scaffolds, respectively). Moreover, it was confirmed that the adherent procedure did not reduce the toughness (figure 3(C)) and revealed significant effect on tensile strength (Figure 3(B)) ($p > 0.05$). According to figures 3(C) and (D), the toughness and elastic modulus of the three-layered scaffold significantly promoted compared to aligned fibrous AP-Gr scaffold (8.125 ± 3.48 MPa and 17.75 ± 5.31 MPa, respectively) and ESM-PCLF membrane (10.59 ± 1.11 MPa and 6.41 ± 0.62 MPa, respectively) ($p > 0.05$). Our results confirmed that the melted PCL layer could not only successfully bond two membranes, but also yielded in enhanced elastic modulus and toughness (29.45 ± 2.08 MPa and 16.91 ± 1.88 MPa). The mechanism suggested for the mechanical behavior of three-layered scaffold was schematically presented in figure 3(E). The application of force in two ends of the three-layered scaffolds resulted in the beneath layers of AP-Gr fibers adhere perfectly to PCL membrane and withstand the stress. This phenomenon resulted in the transfer of force to the PCL membrane and ESM-PCL double network scaffold leading to improvement of the mechanical strength. As demonstrated in previous research, the tensile strength of native nerve trunk is about 12 MPa (Moe *et al* 1992), whereas the tensile strength

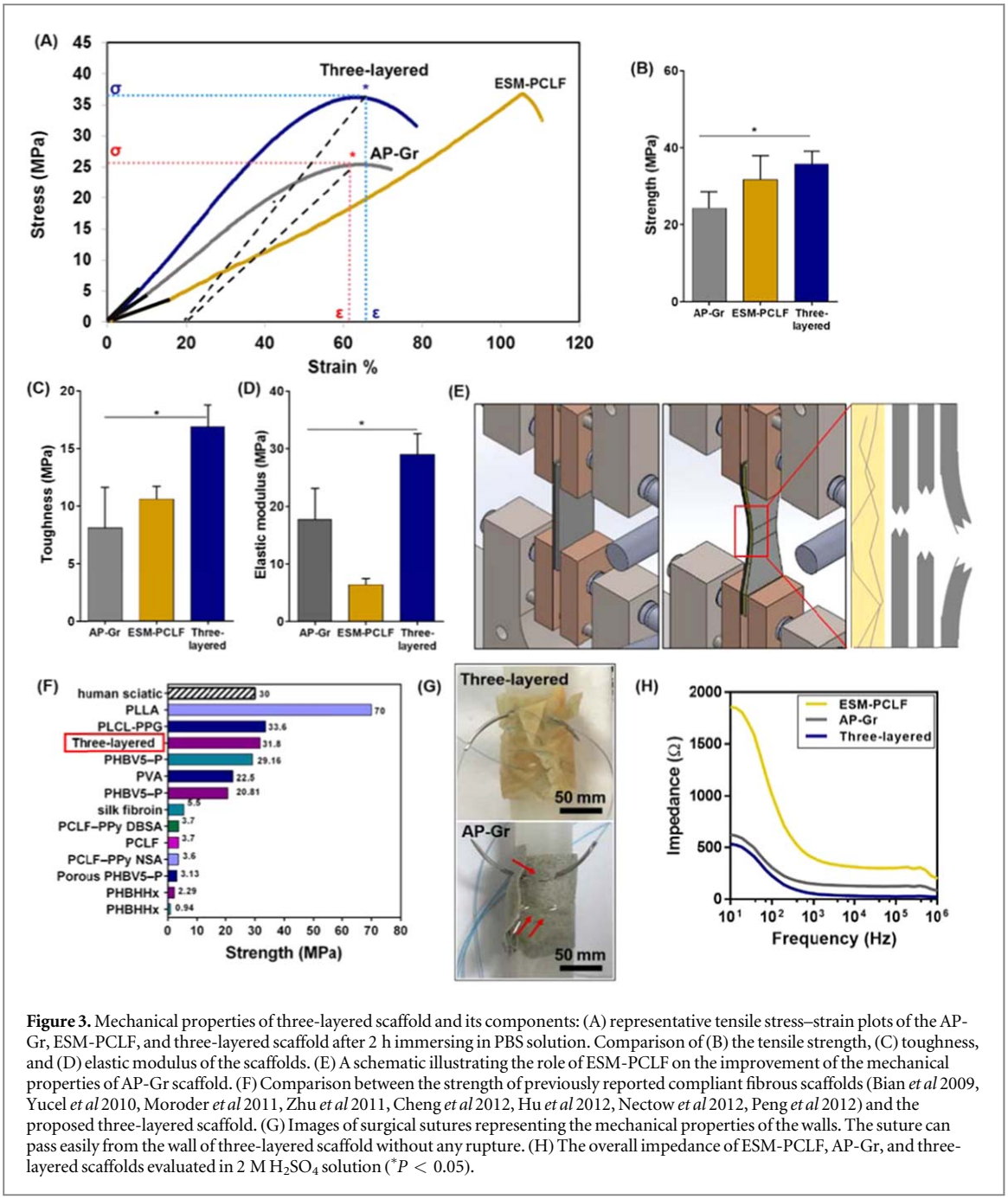

Figure 3. Mechanical properties of three-layered scaffold and its components: (A) representative tensile stress–strain plots of the AP-Gr, ESM-PCLF, and three-layered scaffold after 2 h immersing in PBS solution. Comparison of (B) the tensile strength, (C) toughness, and (D) elastic modulus of the scaffolds. (E) A schematic illustrating the role of ESM-PCLF on the improvement of the mechanical properties of AP-Gr scaffold. (F) Comparison between the strength of previously reported compliant fibrous scaffolds (Bian *et al* 2009, Yucel *et al* 2010, Moroder *et al* 2011, Zhu *et al* 2011, Cheng *et al* 2012, Hu *et al* 2012, Nectow *et al* 2012, Peng *et al* 2012) and the proposed three-layered scaffold. (G) Images of surgical sutures representing the mechanical properties of the walls. The suture can pass easily from the wall of three-layered scaffold without any rupture. (H) The overall impedance of ESM-PCLF, AP-Gr, and three-layered scaffolds evaluated in 2 M H_2SO_4 solution ($^*P < 0.05$).

of three-layered scaffolds was about 30 MPa. It needs to mention that, the mechanical properties of polymers such as sodium alginate and PCLF were affected by temperature and reduced at higher temperature (Moe *et al* 1992, Jayabalan 2009, Masoumi *et al* 2014).

Figure 3(F) presents the mechanical properties of the three-layered scaffolds compared to other scaffolds applied in peripheral nerve tissue engineering (Bian *et al* 2009, Yucel *et al* 2010, Moroder *et al* 2011, Zhu *et al* 2011, Cheng *et al* 2012, Hu *et al* 2012, Nectow *et al* 2012, Peng *et al* 2012). Moreover, according to the previous findings (Peng *et al* 2012), the strength of normal human sciatic nerve tensile properties is about 30 MPa. Ding *et al* (2010) developed chitosan nerve guidance conduit inserted with longitudinal polylactic acid (PLLA) fibers as lumen fillers. In this research, the mismatch between the tensile strength of PLLA (64.3–69.8 MPa) and that of nerve cable was overcome via incorporation of chitosan. So, our results revealed that, the strength of three-layered scaffold was the nearest compared to those of the native nerve trunk. Therefore, thanks to appropriate mechanical properties of multi-layered scaffold, the three-layered tubular construct made of AP-Gr and ESM-PCLF was more robust and tear-resistant during surgical procedures than AP-Gr tubular structure (figure 3(G)). The AP-Gr scaffolds did not reveal great tear resistant against suture and after two passes of needle, the wall of fibers ruptured (detected by red arrows in the figure). In

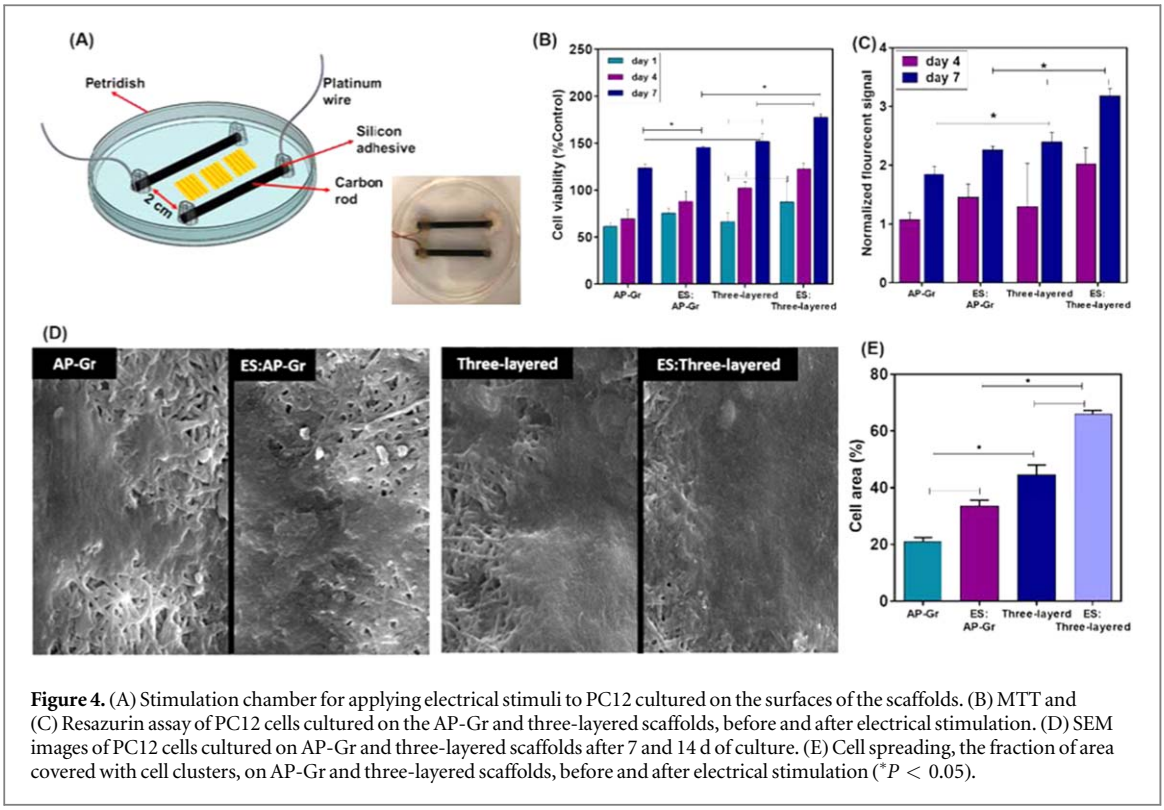

Figure 4. (A) Stimulation chamber for applying electrical stimuli to PC12 cultured on the surfaces of the scaffolds. (B) MTT and (C) Resazurin assay of PC12 cells cultured on the AP-Gr and three-layered scaffolds, before and after electrical stimulation. (D) SEM images of PC12 cells cultured on AP-Gr and three-layered scaffolds after 7 and 14 d of culture. (E) Cell spreading, the fraction of area covered with cell clusters, on AP-Gr and three-layered scaffolds, before and after electrical stimulation ($^{*}P < 0.05$).

contrary, the three-layered tubular scaffold revealed more resistant and the suture could be passed three of times in the wall of scaffold without any rupture.

Electrical conductance is one of the most significant properties for neural regeneration which could be achieved by using conductive nanoparticle (Golafshan *et al* 2017b, Zou *et al* 2016). With respect to the electrical properties of the three-layered scaffolds in figure 3(H), conductivity of the scaffolds was enhanced through the attaching two other scaffolds. Moreover, the three-layered scaffold revealed low impedance value compared to ESM-PCL and AP-Gr. The impedance analysis (figure 3(H)) demonstrated that due to the presence of AP-Gr membrane, the three-layered scaffolds represented low impedance at physiologically relevant frequencies 20 Hz (37.64 ± 0.4 Ω). In a similar research, it was demonstrated that the addition of carbon nanotubes enhance the conductivity of poly(L/D-lactic acid) (PLDLA) matrix from 10^{-13} S cm^{-1} to 10^{-5}–10^{-6} S cm^{-1} (Ahn *et al* 2015).

3.2. *In vitro* biological properties of the three-layered scaffold

The viability of PC12 cells cultured on the three-layered scaffold, was evaluated by MTT assay. Moreover, effect of electrical stimulation on the cell viability was also investigated. Figure 4(A) shows the electrical stimulation chamber developed in this research, schematically. To accomplish electrical stimulation (Annabi *et al* 2013), a set-up consisted of a 8 cm petri-dish and two carbon rod electrodes which the copper wire were rolled at the opposite end of the electrodes and were fixed by silicon adhesive was used. Two electrodes were fixed in petri-dish with the 2 cm distance from each other. In this procedure, the cell-seeded samples were placed between two carbon rods in incubator and the electrical stimulation was applied with the current about 0.02–0.03 A. The viability of PC12 cells on the AP-Gr and three-layered scaffolds was estimated using MTT assay, before and after electrical stimulation (figure 5(B). Results showed that the viability of cells cultured on the various samples enhanced with increasing culture time, confirming that all samples were not cytotoxic. Moreover, compared to control (TCP), the viability of cells cultured on the samples for 7 d was significantly enhanced confirming the effective role of physical and mechanical properties of the substrates on the cell proliferation. Before electrical stimulation, the viability of cells on AP-Gr improved after 7 d and reached to 123.54 ± 4.56 (% control) from 61.59 ± 4.09 (% control). After electrical stimulation, the proliferation of cells significantly enhanced from 75.56 ± 5.67 (% control) to 145.75 ± 1.12 (% control) (for AP-Gr scaffolds) ($p < 0.05$) demonstrating that electrical stimulation had positive effect on PC12 outgrowth. Similar results were detected for three-layered scaffolds. After electrical stimulation, the proliferation of PC12 cells seeded on three-layered construct significantly improved ($p < 0.05$) from 66.83 ± 9.39 (% control) at day 1 to 177.63 ± 3.48 (% control) at day 7 of culture. Similar findings were reported in other researches in which PPy was used as a nerve guidance conduit (Kotwal and Schmidt 2001). Electrical stimulation could influence the growth of PC12 cells owing

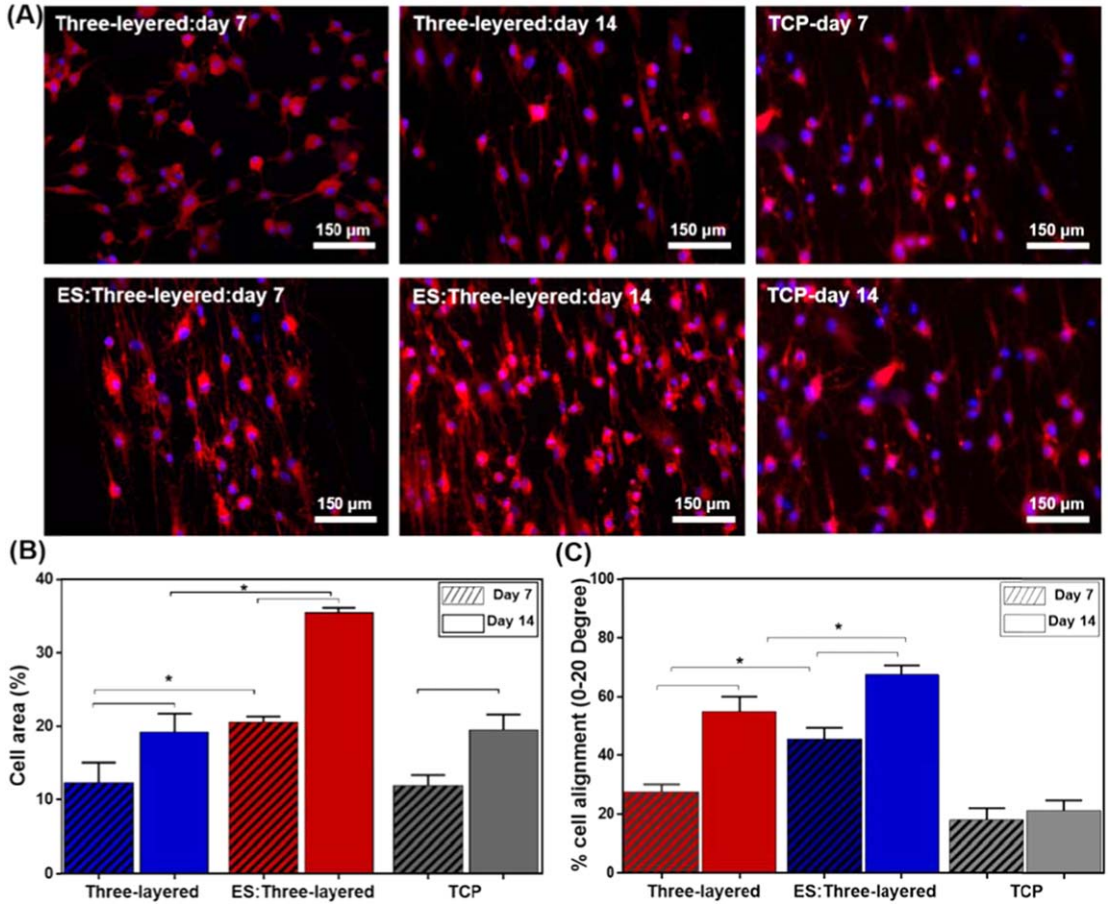

Figure 5. (A) Fluorescence images of the actin cytoskeleton of the PC12 cells on three-layered scaffold and control (TCP) sample after 7 d and 14 d of culture, before and after electrical stimulation (scale bar 150 μm). (B) Proliferation of PC12 cells on the three-layered scaffold and TCP, before and after electrical stimulation. (C) Percentage of cells having orientation angles within 0°–20° angles ($^{*}P < 0.05$).

to the activation of several signaling pathways (Love *et al* 2017). Previous studies have shown that electrical stimulation enhanced the rate of cell proliferation (Kotwal and Schmidt 2001, Prabhakaran *et al* 2011).

The metabolic activity of PC12 cells was also evaluated by Resazurin assay at days 1, 4, and 7 of culture and after electrical stimulation. According to figure 4(C), the proliferation of PC12 cells on the various scaffolds including AP-Gr and three-layered scaffolds enhanced after 7 d of culture. According to figure 4(C), after 7 d of culture, the three-layered scaffold revealed the highest level of fluorescent signal (2.39 ± 0.16) confirming the simultaneous role of mechanical and structural properties on PC12 proliferation compared to AP-Gr scaffolds (1.8 ± 0.1). Furthermore, significant differences were found between the metabolic activity of PC12 seeded on all samples including AP-Gr and three-layered scaffolds, before and after electrical stimulation ($P < 0.05$). Similar results were demonstrated in similar researches which assessed that proliferation of PC12 cells on the various surfaces depended on the micro-architecture, the stiffness, and the biochemical composition of a given substrate (Hartmann *et al* 2013). Moreover, by applying electrical stimulation, the cell proliferation enhanced, significantly. The metabolic activity of PC12 cells on electrical stimulated three-layered scaffold (ES:three-layered scaffold) after 4 d and 7 d of culturing were 2.26 ± 0.7 and 3.2 ± 0.1, respectively, which was significantly more than that of on ES:AP-Gr (1.45 ± 0.2 and 2.3 ± 0.1, respectively) ($p < 0.05$). The effect of electrical stimulation on the proliferation of PC12 cells were similarly studied in previous researches (Aznar-Cervantes *et al* 2017, Ostrovidov *et al* 2017). The SEM images of AP-Gr and three-layered scaffolds after 7 d and 14 d of culture (figure 4(D)) showed that PC12 cells were spread approximately parallel to the direction of fibers and had flattened across a number of fibers for AP-Gr and the three-layered scaffold. Furthermore, the SEM images approved the role of electrical stimulation on the cell proliferation. The SEM images showed that the area covered by PC12 cells were 21.1% ± 1.4%, 33.5% ± 2.1% and 44.5% ± 3.5%, 65.9% ± 1.3% on the AP-Gr, ES:AP-Gr and three-layered and ES:three-layered scaffolds, respectively ($p < 0.05$). These significant differences between the percentage of attached PC12 cells suggested that the features of the scaffolds such as mechanical properties and electrical stimulation could control the spreading of the PC12

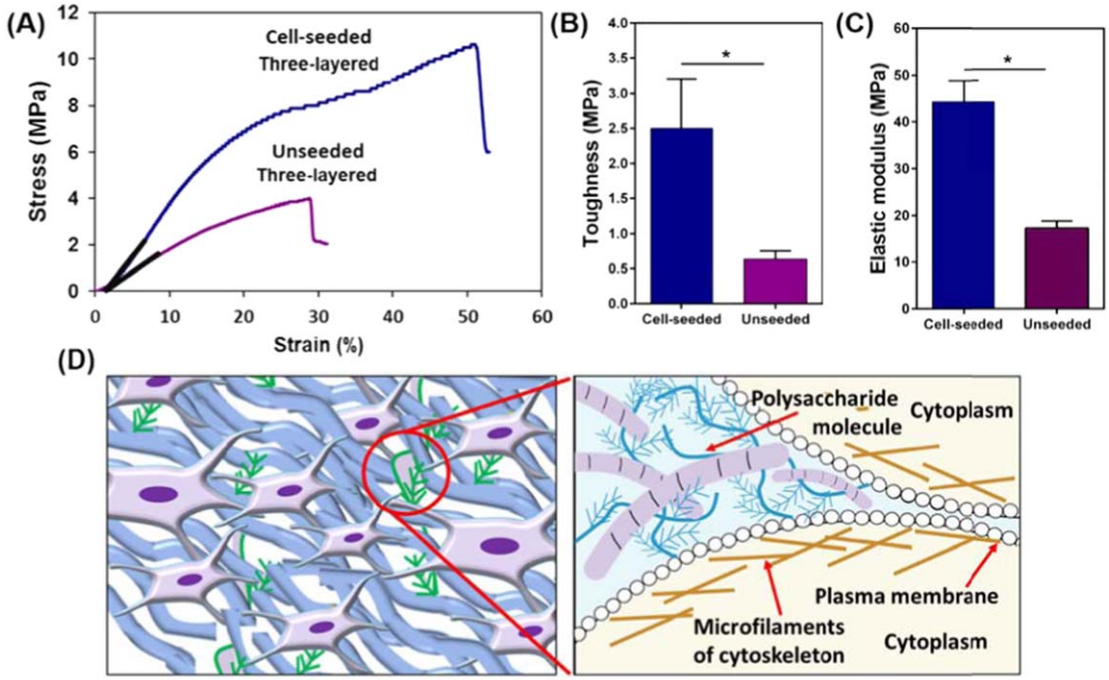

Figure 6. (A) Uniaxial mechanical testing of the unseeded and seeded scaffolds after 14 d immersing in complete media. The comparison between (B) toughness and (C) elastic modulus of the unseeded and seeded three-layered scaffolds ($^{*}P < 0.05$). (D) An illustration of the formation and the role of ECM in improvement the mechanical properties of the scaffolds after 14 d of culturing.

cells. Such these findings reported in similar research showing that fiber orientation of poly (lactic acid) (PLA) and PPy could determine the cell elongation (Tian *et al* 2016). In another research, it was revealed that electrical stimulation enhanced the cell adhesion and proliferation on PPy/PLLA substrates 10 folds more than the control sample (Shi *et al* 2008).

Moreover, we investigated cytoskeletal organization (F-actin) of PC12 cells on the three-layered scaffold, before and after electrical stimulation, and TCP to study the role of electrical stimulation and the substrate structure on the cell morphology. Actin filament staining showed that the cytoskeletal organization of the cells were considerably affected by the scaffold structure, electrical stimulation and culture time. According to figure 5, the cells on the three-layered scaffolds aligned their cytoskeletal structure along the fibers by contact guidance mechanism. In contrast, the cells on TCP were crowded and displayed clustered shape. PC12 cell proliferation was also evaluated with the direct cell counting method at days 7 and 14 of culture. According to figure 5(B) after 14 d of culture, 1.5 times more cells proliferated on the surface of three-layered scaffold (19.23% ± 2.47%) than that of after 7 d of culture (12.32% ± 2.74%). This higher proliferation might be due to the structural and chemical properties of substrates which promote cell growth during 14 d of culturing.

In order to mimic the bioelectricity of the human bodies which maintain the normal biological functions such as signaling of the nervous system (Shi *et al* 2008), the electrical stimulation was performed. After electrical stimulation (figure 5(a)), morphological changes in cells subjected to electrical stimulation could be detected compared to non-electrical stimulated samples and control that were not exposed to any stimulation. While PC12 cells were detected rounded morphology, more and longer neurites could be detected when electrical stimulation was applied. Moreover, after 7 d and 14 d of culture, the cell proliferation was 20.53% ± 0.81% and 35.44% ± 0.64% (control) on the three-layered scaffold which was 1.7 and 1.8 times greater than on the non-stimulated scaffolds, respectively. Similar results reported in another research in which PC12 cells grew on PCLF–polypyrrole (PCLF–PPy) scaffolds and extending neurites were observed parallel to the direction of the applied current (Moroder *et al* 2011).

We further quantified cell alignment on the three-layered scaffold and TCP (figure 5(C)). According to figure 5(C), a larger proportion of the PC12 cells aligned within the 0°–20° preferred angle range as opposed to the control substrate after 14 d of culture. For instance, 55% ± 5% of PC12 cells were oriented in 0°–20° which was significantly more than the number of cells aligned after 7 d of culture (28% ± 2%). After electrical stimulation, the actin fibers of cells were oriented parallel to the fiber direction and showed a more elongated spindle-like morphology compared to the non-electrical stimulated and control samples. These findings indicated that the substrate topography and electrical stimulation affected the cell morphology along with cellular alignment.

Moreover, the fabricated three-layered scaffolds were seeded with PC12 cells for 14 d and the mechanical properties of the seeded and unseeded scaffolds were tested. Before mechanical testing, unseeded scaffolds were submerged in complete media for 14 d in incubator. According to the figure 6(A), strength and elongation of the three-layered scaffold were significantly promoted. Moreover, according to figure 6(B), the toughness of cell-seeded scaffold was four times greater than unseeded scaffold (0.63 ± 4.5 MPa). Furthermore, the elastic modulus of cell-seeded scaffold (figure 6(C)) promoted from 17.33 ± 1.5 MPa (for unseeded scaffold) to 44.33 ± 4.5 MPa (for cell-seeded scaffold). According to figure 6(D), the significant changes in mechanical properties of the scaffolds could be due to the production of ECM proteins by the cells on the three-layered scaffolds. As prepared ECM could provide structural and mechanical support for tissue integrity and maintained cell attachment, growth and shaping of cells into tissues. According to figure 6(D), ESM consisted of fibrous proteins consisting of collagen and elastin with crucial tensile strength, enabling resistance to plastic deformation and rupture and supporting tissues to resist repetitive mechanical stress (Muiznieks and Keeley 2013). Moreover, the low mechanical properties of the unseeded three-layered scaffold might be due to the degradation of the scaffold. These results were in accordance with other studies indicating the effect of cell seeding and formation of ESM and collagen secretion on the scaffolds (Engelmayr *et al* 2005, Masoumi *et al* 2014).

4. Conclusion

In present work, we have developed a three-layered scaffold made of three layers (AP-Gr (inner layer), PCL (middle layer) and ESM-PCLF (outer layer)). This scaffold was biodegradable, mechanically robust, conductive, flexible and easy to handle. The three-layered scaffold was seeded with PC12 cells that aligned along the parallel structure of inner layer (AP-Gr). We notably highlighted that each of these cues acted positively and additionally on nerve cell proliferation and orientation. For instance, the proliferation of PC12 cells seeded on the three-layered scaffolds was significantly enhanced (1.5 times) compared to AP-Gr scaffold. Overall, the three-layered scaffold with tunable mechanical and biological properties would potentially be a promising candidate for the regeneration of nerve tissue.

Acknowledgments

The authors are grateful for support of this research by Dr Sahar Salehi.

ORCID iDs

Mahshid Kharaziha https://orcid.org/0000-0002-8803-105X
Morteza Alehosseini https://orcid.org/0000-0001-8298-9139

References

Ahn H-S, Hwang J-Y, Kim M S, Lee J-Y, Kim J-W, Kim H-S, Shin U S, Knowles J C, Kim H-W and Hyun J K 2015 Carbon-nanotube-interfaced glass fiber scaffold for regeneration of transected sciatic nerve *Acta Biomater.* **13** 324–34

Alehosseini M, Golafshan N, Kharaziha M, Fathi M and Edris H 2018 Hemocompatible and bioactive heparin-loaded PCL-α-TCP fibrous membranes for bone tissue engineering *Macromol. Biosci.* **18** 1800020

Amini N, Kalaee M, Mazinani S, Pilevar S and Ranaei-Siadat S-O 2013 Morphological optimization of electrospun polyacrylamide/MWCNTs nanocomposite nanofibers using Taguchi's experimental design *Int. J. Adv. Manuf. Technol.* **69** 139–46

Annabi N, Tsang K, Mithieux S M, Nikkhah M, Ameri A, Khademhosseini A and Weiss A S 2013 Highly elastic micropatterned hydrogel for engineering functional cardiac tissue *Adv. Funct. Mater.* **23** 4950–9

Aznar-Cervantes S, Pagán A, Martínez J G, Bernabeu-Esclapez A, Otero T F, Meseguer-Olmo L, Paredes J I and Cenis J L 2017 Electrospun silk fibroin scaffolds coated with reduced graphene promote neurite outgrowth of PC-12 cells under electrical stimulation *Mater. Sci. Eng.* C **79** 315–25

Balaz M 2014 Eggshell membrane biomaterial as a platform for applications in materials science *Acta Biomater.* **10** 3827–43

Bian Y Z, Wang Y, Aibaidoula G, Chen G Q and Wu Q 2009 Evaluation of poly(3-hydroxybutyrate-co-3-hydroxyhexanoate) conduits for peripheral nerve regeneration *Biomaterials* **30** 217–25

Cheng H K, Sahoo N G, Tan Y P, Pan Y, Bao H, Li L, Chan S H and Zhao J 2012 Poly(vinyl alcohol) nanocomposites filled with poly(vinyl alcohol)-grafted graphene oxide *ACS Appl. Mater. Interfaces* **4** 2387–94

Ding F, Wu J, Yang Y, Hu W, Zhu Q, Tang X, Liu J and Gu X 2010 Use of tissue-engineered nerve grafts consisting of a chitosan/poly (lactic-co-glycolic acid)-based scaffold included with bone marrow mesenchymal cells for bridging 50 mm dog sciatic nerve gaps *Tissue Eng.* A **16** 3779–90

Engelmayr G C, Rabkin E, Sutherland F W, Schoen F J, Mayer J E and Sacks M S 2005 The independent role of cyclic flexure in the early *in vitro* development of an engineered heart valve tissue *Biomaterials* **26** 175–87

Golafshan N, Gharibi H, Kharaziha M and Fathi M 2017a A facile one-step strategy for development of a double network fibrous scaffold for nerve tissue engineering *Biofabrication* **9** 025008

Golafshan N, Kharaziha M and Fathi M 2017b Tough and conductive hybrid graphene-PVA: alginate fibrous scaffolds for engineering neural construct *Carbon* **111** 752–63

Golafshan N, Kharaziha M, Fathi M, Larson B L, Giatsidis G and Masoumi N 2018 Anisotropic architecture and electrical stimulation enhance neuron cell behaviour on a tough graphene embedded PVA: alginate fibrous scaffold *RSC Adv.* **8** 6381–9

Golafshan N, Rezahasani R, Esfahani M T, Kharaziha M and Khorasani S 2017c Nanohybrid hydrogels of laponite: PVA-Alginate as a potential wound healing material *Carbohydrate Polymers* **176** 392–401

Hartmann H, Hossfeld S, Schlosshauer B, Mittnacht U, Pego A P, Dauner M, Doser M, Stoll D and Krastev R 2013 Hyaluronic acid/chitosan multilayer coatings on neuronal implants for localized delivery of siRNA nanoplexes *J. Control. Release* **168** 289–97

Hu C, Uchida T, Tercero C, Ikeda S, Ooe K, Fukuda T, Arai F, Negoro M and Kwon G 2012 Development of biodegradable scaffolds based on magnetically guided assembly of magnetic sugar particles *J. Biotechnol.* **159** 90–8

Isaacs J and Browne T 2014 Overcoming short gaps in peripheral nerve repair: conduits and human acellular nerve allograft *Hand* **9** 131–7

Jayabalan M 2009 Studies on poly(propylene fumarate-co-caprolactone diol) thermoset composites towards the development of biodegradable bone fixation devices *Int. J. Biomater.* **2009** 486710

Jiang X, Mi R, Hoke A and Chew S Y 2014 Nanofibrous nerve conduit-enhanced peripheral nerve regeneration *J. Tissue Eng. Regen. Med.* **8** 377–85

Kakinoki S, Nakayama M, Moritan T and Yamaoka T 2014 Three-layer microfibrous peripheral nerve guide conduit composed of elastin-laminin mimetic artificial protein and poly(L-lactic acid) *Frontiers Chem.* **2** 52

Khorshidi S, Solouk A, Mirzadeh H, Mazinani S, Lagaron J M, Sharifi S and Ramakrishna S 2016 A review of key challenges of electrospun scaffolds for tissue-engineering applications *J. Tissue Eng. Regen. Med.* **10** 715–38

Kotwal A and Schmidt C E 2001 Electrical stimulation alters protein adsorption and nerve cell interactions with electrically conducting biomaterials *Biomaterials* **22** 1055–64

Lackington W A, Ryan A J and O'brien F J 2017 Advances in nerve guidance conduit-based therapeutics for peripheral nerve repair *ACS Biomater. Sci. Eng.* **3** 1221–35

Lee B-K, Ju Y M, Cho J-G, Jackson J D, Lee S J, Atala A and Yoo J J 2012 End-to-side neurorrhaphy using an electrospun PCL/collagen nerve conduit for complex peripheral motor nerve regeneration *Biomaterials* **33** 9027–36

Li N, Zhang Q, Gao S, Song Q, Huang R, Wang L, Liu L, Dai J, Tang M and Cheng G 2013 Three-dimensional graphene foam as a biocompatible and conductive scaffold for neural stem cells *Sci. Rep.* **3** 1604

Lin Y-L, Jen J-C, Hsu S-H and Chiu M 2008 Sciatic nerve repair by microgrooved nerve conduits made of chitosan-gold nanocomposites *Surgical Neurol.* **70** S9–18

Liu X, Miller A L, Park S, Waletzki B E, Zhou Z, Terzic A and Lu L 2017 Functionalized carbon nanotube and graphene oxide embedded electrically conductive hydrogel synergistically stimulates nerve cell differentiation *ACS Appl. Mater. Interfaces* **9** 14677–90

Loh Q L and Choong C 2013 Three-dimensional scaffolds for tissue engineering applications: role of porosity and pore size *Tissue Eng.* B **19** 485–502

Love M R, Palee S, Chattipakorn S C and Chattipakorn N 2017 Effects of Electrical Stimulation on Cell Proliferation and Apoptosis *J. Cell. Physiol.* **233** (3) 1860–76

Masoumi N, Annabi N, Assmann A, Larson B L, Hjortnaes J, Alemdar N, Kharaziha M, Manning K B, Mayer J E and Khademhosseini A 2014 Tri-layered elastomeric scaffolds for engineering heart valve leaflets *Biomaterials* **35** 7774–85

Mekaj A Y, Morina A A, lajQi S, Manxhuka-kerliu S, Kelmendi F M and Duci S B 2015 Biomechanical properties of the sciatic nerve following repair: effects of topical application of hyaluronic acid or tacrolimus *Int. J. Clin. Exp. Med.* **8** 20218

Moe S T, Draget K I, Skjåk-bræk G and Simdsrød O 1992 Temperature dependence of the elastic modulus of alginate gels *Carbohydrate Polym.* **19** 279–84

Moroder P, runge M B, wang H, ruesink T, Lu L, Spinner R J, Windebank A J and Yaszemski M J 2011 Material properties and electrical stimulation regimens of polycaprolactone fumarate-polypyrrole scaffolds as potential conductive nerve conduits *Acta Biomater.* **7** 944–53

Mottaghitalab F, Farokhi M, Zaminy A, Kokabi M, Soleimani M, Mirahmadi F, Shokrgozar M A and Sadeghizadeh M 2013 A biosynthetic nerve guide conduit based on silk/SWNT/fibronectin nanocomposite for peripheral nerve regeneration **8** (10) e74417

Muiznieks L D and Keeley F W 2013 Molecular assembly and mechanical properties of the extracellular matrix: a fibrous protein perspective *Biochim. Biophys. Acta-Mol. Basis Dis.* **1832** 866–75

Naghavi Alhosseini S, Moztarzadeh F, Kargozar S, Dodel M and Tahriri M 2015 Development of polyvinyl alcohol fibrous biodegradable scaffolds for nerve tissue engineering applications:in vitrostudy *Int. J. Polym. Mater. Polym. Biomater.* **64** 474–80

Nectow A R, Marra K G and Kaplan D L 2012 Biomaterials for the development of peripheral nerve guidance conduits *Tissue Eng.* B **18** 40–50

O'Brien F J 2011 Biomaterials and scaffolds for tissue engineering *Mater. Today* **14** 88–95

Ostrovidov S, Ahadian S, Ramon-Azcon J, Hosseini V, Fujie T, Parthiban S P, Shiku H, Matsue T, Kaji H and Ramalingam M 2017 Three-dimensional co-culture of C2C12/PC12 cells improves skeletal muscle tissue formation and function *J. Tissue Eng. Regen. Med.* **11** 582–95

Peng C, Zhang Q, Yang Q and Zhu Q 2012 Strain and stress variations in the human amniotic membrane and fresh corpse autologous sciatic nerve anastomosis in a model of sciatic nerve injury *Neural Regener. Res.* **7** 1779

Prabhakaran M P, Ghasemimobarakeh L, Jin G and Ramakrishna S 2011 Electrospun conducting polymer nanofibers and electrical stimulation of nerve stem cells *J. Biosci. Bioeng.* **112** 501–7

Ryan A J, Lackington W A, Hibbitts A J, Matheson A, Alekseeva T, Stejskalova A, Roche P and O'brien F J 2017 A physicochemically optimized and neuroconductive biphasic nerve guidance conduit for peripheral nerve repair *Adv. Healthcare Mater.* **6** 1700954

Shi G, Zhang Z and rouabhia M 2008 The regulation of cell functions electrically using biodegradable polypyrrole–polylactide conductors *Biomaterials* **29** 3792–8

Sulong A F, Hassan N H, Hwei N M, Lokanathan Y, Naicker A S, Abdullah S, Yusof M R, Htwe O, Idrus R and Haflah N 2014 Collagen-coated polylactic-glycolic acid (PLGA) seeded with neural-differentiated human mesenchymal stem cells as a potential nerve conduit *Adv. Clin. Exp. Med.* **23** 353–62

Tian L, Prabhakaran M P, Hu J, Chen M, Besenbacher F and Ramakrishna S 2016 Synergistic effect of topography, surface chemistry and conductivity of the electrospun nanofibrous scaffold on cellular response of PC12 cells *Colloids Surfaces* B **145** 420–9

Wang S, Yaszemski M J, Gruetzmacher J A and Lu L 2008 Photo-crosslinked poly (ε-caprolactone fumarate) networks: roles of crystallinity and crosslinking density in determining mechanical properties *Polymer* **49** 5692–9

Wang S, Yaszemski M J, Knight A M, Gruetzmacher J A, Windebank A J and Lu L 2009 Photo-crosslinked poly (ε-caprolactone fumarate) networks for guided peripheral nerve regeneration: material properties and preliminary biological evaluations *Acta Biomater.* **5** 1531–42

Xie J, Macewan M R, Liu W, Jesuraj N, Li X, Hunter D and Xia Y 2014 Nerve guidance conduits based on double-layered scaffolds of electrospun nanofibers for repairing the peripheral nervous system *ACS Appl. Mater. Interfaces* **6** 9472–80

Yucel D, Kose G T and Hasirci V 2010 Polyester based nerve guidance conduit design *Biomaterials* **31** 1596–603

Zhang K, Zheng H, Liang S and Gao C 2016 Aligned PLLA nanofibrous scaffolds coated with graphene oxide for promoting neural cell growth *Acta Biomater.* **37** 131–42

Zhu Y, Wang A, Patel S, Kurpinski K, Diao E, Bao X, Kwong G, Young W L and Li S 2011 Engineering bi-layer nanofibrous conduits for peripheral nerve regeneration *Tissue Eng.* C **17** 705–15

Zou Y, Qin J, Huang Z, Yin G, Pu X and He D 2016 Fabrication of aligned conducting PPy-PLLA fiber films and their electrically controlled guidance and orientation for neurites *ACS Appl. Mater. Interfaces* **8** 12576–82